Communication

Photoinduced Site-Selective Aryl C-H Borylation with Electron-Donor-Acceptor Complex Derived from B_2Pin_2 and Isoquinoline

Manhong Li [1,2,3,4,†], Yi-Hui Deng [1,†], Qianqian Chang [2,†], Jinyuan Li [5], Chao Wang [1], Leifeng Wang [2,*] and Tian-Yu Sun [1,3,*]

1   Key Lab of Computational Chemistry and Drug Design, State Key Laboratory of Chemical Oncogenomics, School of Chemical Biology and Biotechnology, Peking University Shenzhen Graduate School, Shenzhen 518055, China; e1328001@u.nus.edu (M.L.); dyh@stu.pku.edu.cn (Y.-H.D.); wangchao@pku.edu.cn (C.W.)

2   School of Pharmaceutical Sciences (Shenzhen), Sun Yat-sen University, No. 66, Gongchang Road, Shenzhen 518107, China; changqq3@mail2.sysu.edu.cn

3   Institute of Molecular Chemical Biology, Shenzhen Bay Laboratory, Shenzhen 518132, China

4   Department of Pharmacy and Pharmaceutical Sciences, Faculty of Science, National University of Singapore, Block S4A, Level 3, 18 Science Drive 4, Singapore 117543, Singapore

5   Shanghai Institute of Organic Chemistry, University of Chinese Academy of Sciences, Chinese Academy of Sciences, 345 Lingling Lu, Shanghai 200032, China; lijinyuan@mail.sioc.ac.cn

*   Correspondence: wanglf33@mail.sysu.edu.cn (L.W.); tian-yu_sun@pku.edu.cn (T.-Y.S.)

†   These authors contributed equally to this work.

Abstract: Due to boron's metalloid properties, aromatic boron reagents are prevalent synthetic intermediates. The direct borylation of aryl C-H bonds for producing aromatic boron compounds offers an appealing, one-step solution. Despite significant advances in this field, achieving regioselective aryl C-H bond borylation using simple and readily available starting materials still remains a challenge. In this work, we attempted to enhance the reactivity of the electron-donor-acceptor (EDA) complex by selecting different bases to replace the organic base (NEt_3) used in our previous research. To our delight, when using NH_4HCO_3 as the base, we have achieved a mild visible-light-mediated aromatic C-H bond borylation reaction with exceptional regioselectivity (rr > 40:1 to single isomers). Compared with our previous borylation methodologies, this protocol provides a more efficient and broader scope for aryl C-H bond borylation through the use of N-Bromosuccinimide. The protocol's good functional-group tolerance and excellent regioselectivity enable the functionalization of a variety of biologically relevant compounds and novel cascade transformations. Mechanistic experiments and theoretical calculations conducted in this study have indicated that, for certain arenes, the aryl C-H bond borylation might proceed through a new reaction mechanism, which involves the formation of a novel transient EDA complex.

Keywords: photocatalysis; C-H bond; borylation; electron-donor-acceptor; B_2Pin_2; isoquinoline

1. Introduction

Aromatic boron reagents are widely used as synthetic intermediates in the production of pharmaceuticals and natural products through Suzuki–Miyaura/Chan-Lam cross-coupling [1–5], oxidation [6], halogenation [7,8] and homologation [9] benefiting from the unique metalloid properties of boron [10–12]. In principle, the direct borylation of aryl C-H bonds for producing aromatic boron compounds offers an appealing, one-step solution compared to traditional strategies [13–16]; however, this approach has proven to be quite challenging.
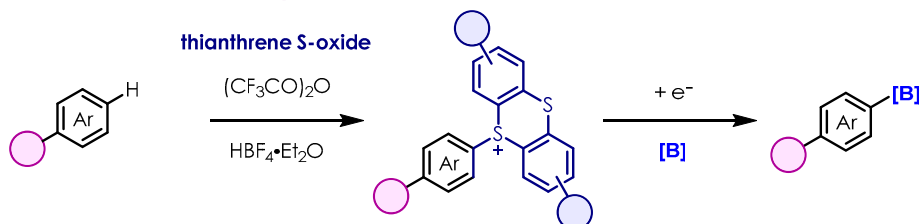
Transition metal-promoted directed C-H bond activation, especially using Ir/Rh, has emerged as a powerful tool for the construction of C-B bonds [17–19] (Scheme 1a), commonly

relying on precious metal catalysts and appropriate directing groups (DG). Moreover, the presence of multiple functional groups in complex bioactive molecules often poses a challenge for their late-stage borylation, particularly under harsh reaction conditions.
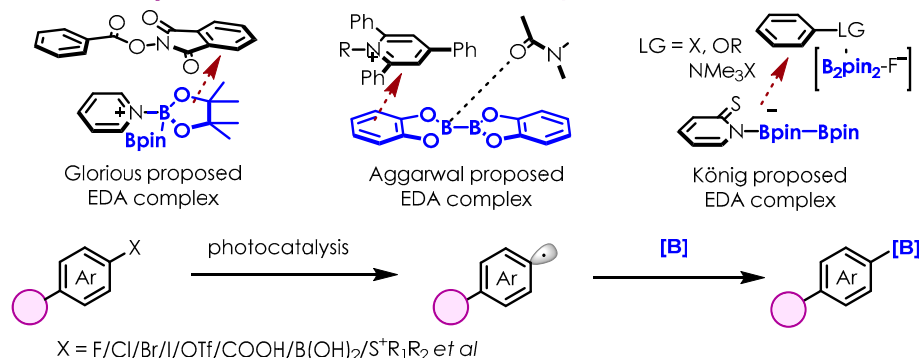
[a] Direct aryl C-H borylation by transition metal catalysis
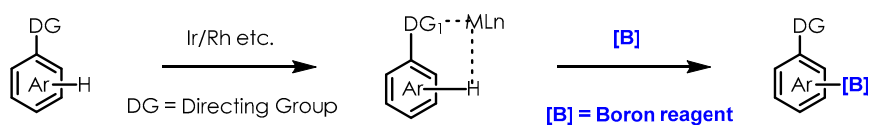
[b] Two-step aryl C-H borylation through thianthrenium salts

[c] Photocatalysis using EDA complex for the borylation of arenes

Glorious proposed
EDA complex

Aggarwal proposed
EDA complex

König proposed
EDA complex

X = F/Cl/Br/I/OTf/COOH/B(OH)$_2$/S$^+$R$_1$R$_2$ *et al*

[d] Our previous work: aryl C-H borylation through *in situ* formed EDA complex

X = Cl or Br
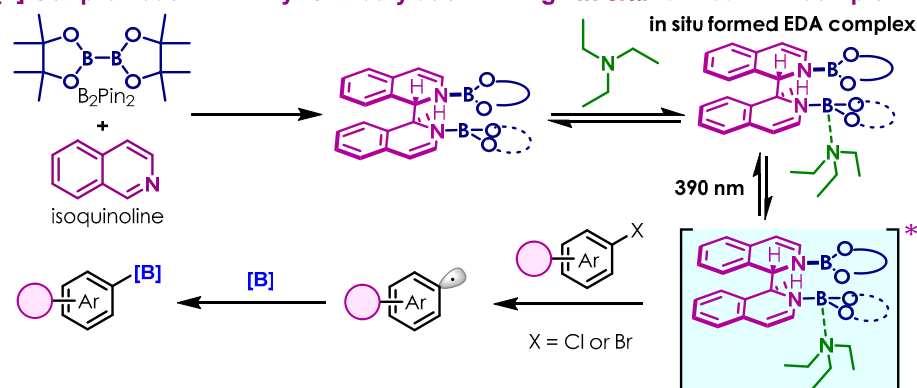
[e] This work: one-step, site selective aryl C-H borylation through our proposed transient EDA complex

selecting different bases

in situ formed EDA complex

transient EDA complex
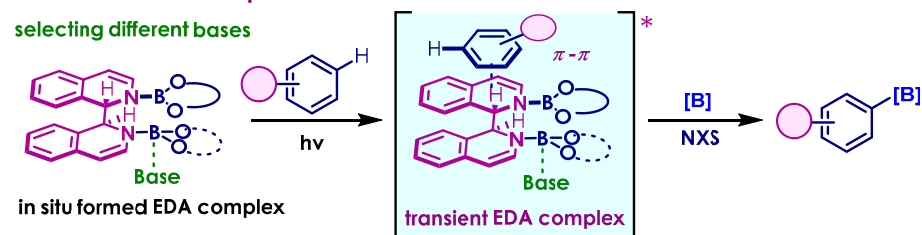
Scheme 1. Synthetic approaches to aryl boronic esters. (The symbol * denotes excited state).

Ritter developed a series of elegant late-stage C-H bond functionalization protocols [20–22] through site-selective thianthrenation, utilizing thianthrene S-oxide as a versatile pre-functionalization reagent. Triggered by a single electron transfer (SET) progress, the C-S bond of aryl thianthrenium salts can be cleaved to form thianthrene and aryl radical [23,24], which is then spontaneously captured by the diboron reagent (Scheme 1b) [25]. Despite these pioneering advancements, achieving regioselective aryl C-H bond borylation using simple and readily available starting materials still remains a challenge.

In recent years, photocatalysis [26–31] using the electron-donor-acceptor (EDA) complex [32–35] has gained popularity, offering new methods for radical-mediated transformations. Due to boron's metalloid properties [10–12], there is increasing interest in using boron reagents as alternatives to prevalent transition metals for photocatalysis. The notably high reactivity of diboron reagents makes them excellent precursors for constructing the EDA complex, as they can effectively combine with electron donor partners, such as amines and N-containing heterocycles (NCHs) (Scheme 1c). Glorius [36] disclosed a photoinduced decarboxylative borylation of aryl N-hydroxyphthalimide esters via the use of Katritzky salts as acceptor in the EDA complex. Aggarwal [37] proposed an EDA complex formed by 2-iodophrnyl thiocarbonate, bis(pinacolato)diboron (B_2Pin_2) and *N,N*-dimethylformamide, resulting in the formation of boronic esters with high stereocontrol. König [38] achieved an ipso-borylation of substituted arenes by utilizing an EDA complex formed between thiolate, B_2Pin_2 and boryl anion activated substrates.

Our group has recently described several strategies for generating aryl radicals under visible-light catalysis [39–41], and our previous studies have demonstrated that the reductive coupling of isoquinoline and B_2Pin_2 can produce a dimer. This dimer can coordinate with an organic base (NEt_3) in situ to form an EDA complex (Scheme 1d). Under visible-light irradiation, the excited state of the in situ-formed EDA complex is a highly active reductant and can facilitate SET with aryl halides to produce aryl radical intermediates [40].

Inspired by our earlier work and other elegant conceptions [42–45], we wonder whether selecting different bases could facilitate the photoinduced formation of a transient EDA complex between the in situ-formed EDA complex and certain arenes through π–π interaction. This transient EDA complex could then undergo direct C-H borylation upon treatment with regioselective oxidative additives (e.g., N-Halosuccinimides/NXS: X = Cl, Br, I) [46,47] (Scheme 1e).

Our mechanistic experiments and theoretical calculations in this study have indicated that, when using NH_4HCO_3 as the base, certain arenes may indeed yield borylation products through the transient EDA complex formation pathway. Furthermore, the yield is significantly increased compared to the organic base (NEt_3) used in our previous work [40]. This research holds the potential to enhance the highly efficient, site-selective, direct C-H borylation of more challenging arenes.
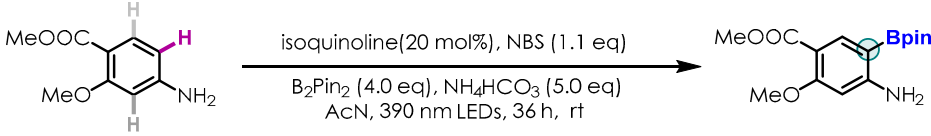
2. Results

2.1. Optimization of Reaction Conditions for the Aryl C-H Bond Borylation

We optimized the reaction conditions for the borylation of methyl 4-amino-2-methoxybenzoate using a mixture of B_2Pin_2, isoquinoline (a N-containing heterocycle, NCH) and a base under visible-light irradiation (Table 1). Extensive screening of the reaction conditions revealed that treating methyl 4-amino-2-methoxybenzoate with NBS (0.22 mmol), isoquinoline (20 mol%), B_2Pin_2 (0.8 mmol), and NH_4HCO_3 in acetonitrile resulted in the borylated product with a 72% NMR yield (68% isolated yield, entry **1**). The choice of the base had a great influence on the efficiency of borylation (entries 2–5). Organic bases such as *N,N*-Diisopropylethylamine (DIEPA) and triethylamine (NEt_3) did not perform well under standard condition compared to NH_4HCO_3 (see Supporting Information Table S1). These results indicate that using NH_4HCO_3 as a base provides a clear advantage over our previous work using organic base (NEt_3) [40]. A total of 2.0 eq NBS led to reduced quantities of the desired product (54%; entry 6). Not surprisingly, no desired product was

observed without the addition of NBS (entry 7). Finally, the photochemical nature of this borylation strategy was confirmed, as the reaction did not occur either in the absence of light (entry 8) or in the absence of the EDA complex precursor (entry 9).

Table 1. Optimization of the reaction conditions [a].

Entry	Deviations from Standard Condition	Yield (%) [b]
1	none	72(68) [c]
2	NEt$_3$ instead of NH$_4$HCO$_3$	31
3	KOH instead of NH$_4$HCO$_3$	trace
4	Cs$_2$CO$_3$ instead of NH$_4$HCO$_3$	54
5	NaHCO$_3$ instead of NH$_4$HCO$_3$	19
6	2.0 eq NBS instead of 1.1 eq NBS	54
7	NO NBS instead of 1.1 eq NBS	0
8	No light	0
9	No isoquinoline	0

[a] Reactions were performed with 0.2 mmol methyl 4-amino-2-methoxybenzoate, 1.0 mmol base, 20 mol% N-containing heterocycle (NCH), 0.8 mmol B$_2$Pin$_2$, and 0.22 mmol NBS in 0.5 mL acetonitrile under 390 nm LEDs irradiation for 36 h. [b] NMR yields using pyrazine or hexamethyl disiloxane as internal standard. [c] Isolated yields.

2.2. Substrate Scope of the Photoinduced Aryl C-H Borylation

Having demonstrated the validity of our proposal, we turned our attention to the substrate scope of arenes utilizing NH$_4$HCO$_3$ as the additive. A variety of aromatic substrates were subjected to the C-H borylation procedure using B$_2$Pin$_2$ as the aryl radical trap in the photochemical progress (Figure 1).

Phenol, aniline, and their electron donating/withdrawing group-protected derivatives (**1**–**14**) were smoothly converted to the corresponding arylboronates in moderate-to-good yields (30–76%), with excellent selectivity for the para-selective products (rr > 40:1 for single isomers). Heterocycles such as morpholine (**15**) and pyrrolidine (**16**) were also competent substrates.

Electron-rich and electron-deficient group di-substituted arenes, such as 1,2-, 1,3-, and 1,4-substituted arenes can also undergo the C-H borylation reaction in moderate-to-good yields (**17**–**32**), showcasing the compatibility of our method with a broad array of functionalities (e.g., difluoromethoxyl-, trifluoromethyl-, trifluoromethoxy-, cyano-, methoxycarbonyl-, cyclohexyl- and naked hydroxyl/amino). A dual borylation product (**28**) was successfully synthesized using boronic ester aniline. Medically relevant fluorine-containing anilines led to C-H borylation products with high efficiencies (**21**, **23**–**26**, **29**).

Of particular note is the capability of this method to regioselectively and efficiently construct the C-B bond from the hindered aryl C-H bond, as shown by the reaction of substrates **33**–**44**, yielding the desired borylation products in good yield and with excellent chemoselectivities.

Remarkably, the borylation reaction of bicyclic aromatic substrates, such as 2,3-dihydrobenzofuran (**45**), chromane (**46**), and 1,2,3,4-tetrahydroisoquinoline derivative (**47**), all proceeded smoothly and afforded the corresponding borylation products as single regio-isomers in accordance with the high reactivity of these positions for electrophilic substitution.

However, thioanisole and strong electron-withdrawing-group substituted arenes were not tolerated. Methyl benzoate and benzonitrile did not deliver the desired products under standard reaction conditions.
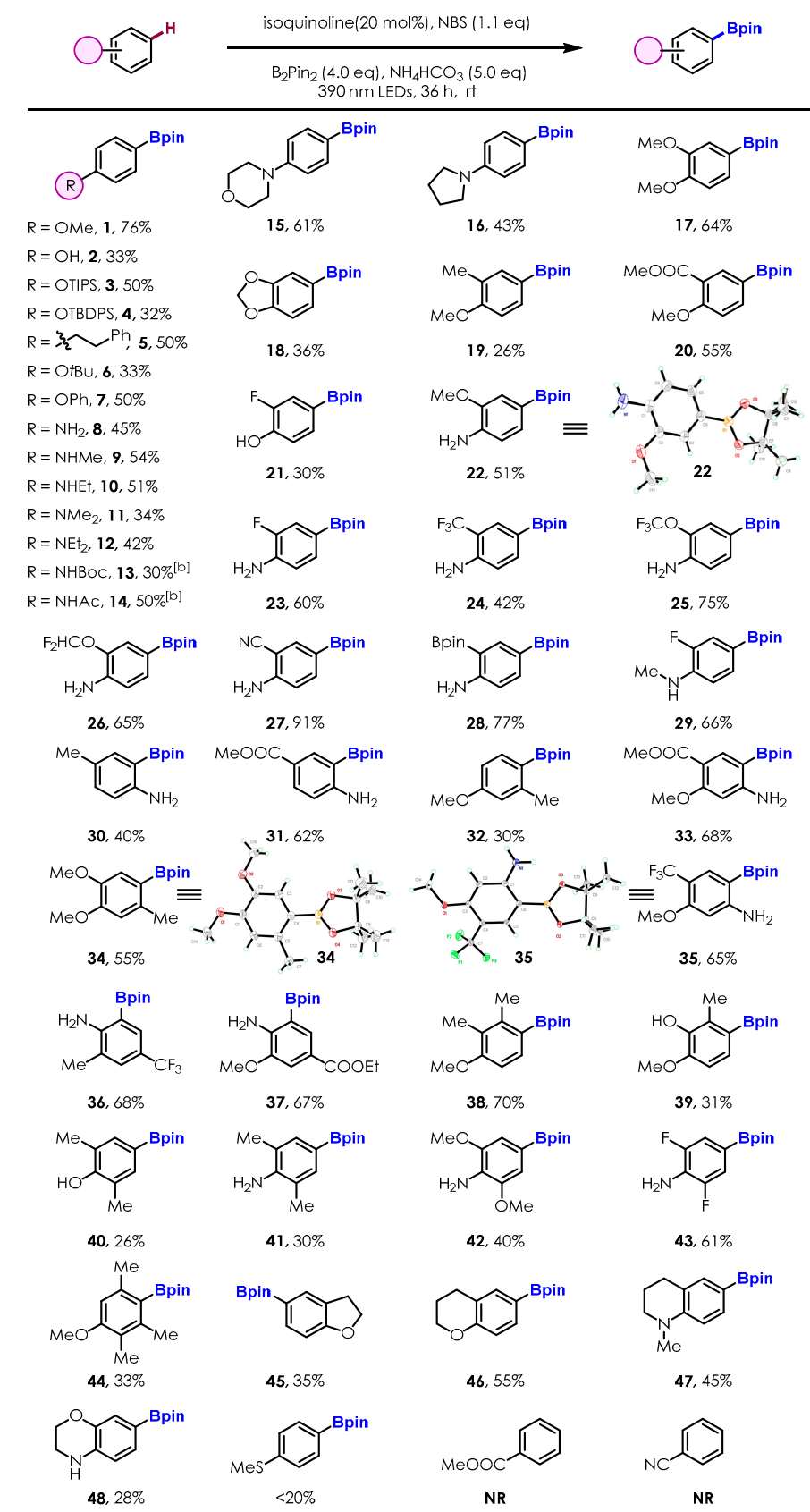
Figure 1. Substrate scope of arenes. Reactions were run on 0.2 mmol scales, isolated yield. [b] 0.2 mmol isoquinoline, 72 h.

The regioselectivity of the C-H borylation reaction is governed by both the electronic and steric effects of the substituents, similar to the nucleophilic substitution reactions induced by triptycenyl sulfide, as reported by Miura and co-workers [46].

2.3. Late-Stage Functionalization and Novel Cascade Transformation

To assess the applicability of this aryl C-H borylation strategy for late-stage functionalization, a variety of representative active pharmaceutical ingredients (APIs) and natural products, including anaesthesine, gemfibrozil, levodropropizine, atomoxetine, and natural phenol thymol, were subjected to this protocol. These compounds were found to be tolerant in this protocol, yielding the corresponding borylated derivatives in good yields in a single-isomer manner (Figure 2). These transformations accommodated various functional groups, including sensitive esters, amides, and N-heterocycles, highlighting the mildness and practicality of this protocol. Notably, this methodology also worked well with a series of diboron reagents to produce gemfibrozil derivatives A–D with useful efficiencies (e.g., **D**, 52% yield).
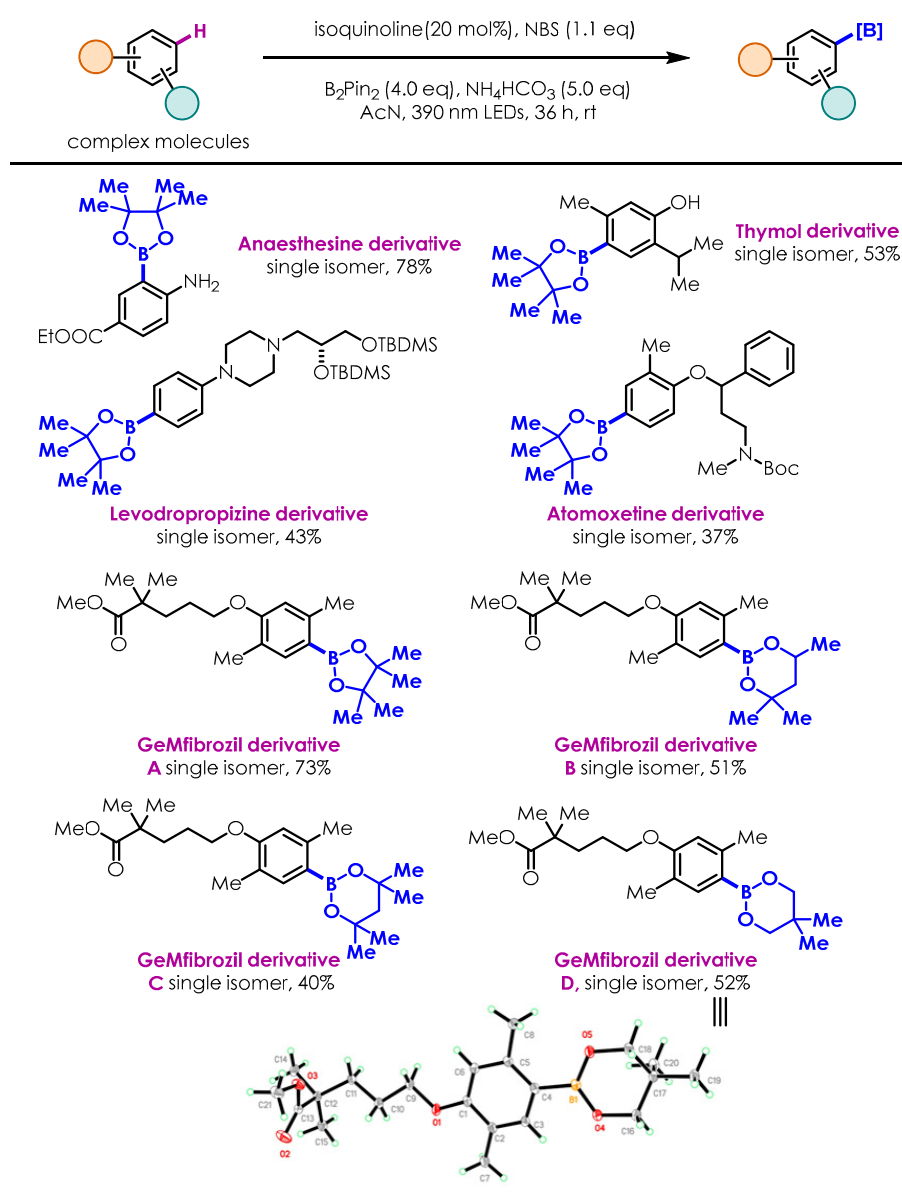

Figure 2. Late-stage functionalization of complex molecules. Reactions were run on 0.2 mmol scales, isolated yield.

To further demonstrate the utility of this novel borylation protocol (Figure 3), more challenging cascade transformations were studied. Reductive cleavages of unusual N-N/C-O bonds and detosylation followed by direct C-H bond borylation under standard conditions afforded the borylated aniline and phenol derivatives with good efficiencies. Each of these transformations is highly important, as site-selective cascade transformation of the aromatic C-H bond remains a major challenge.
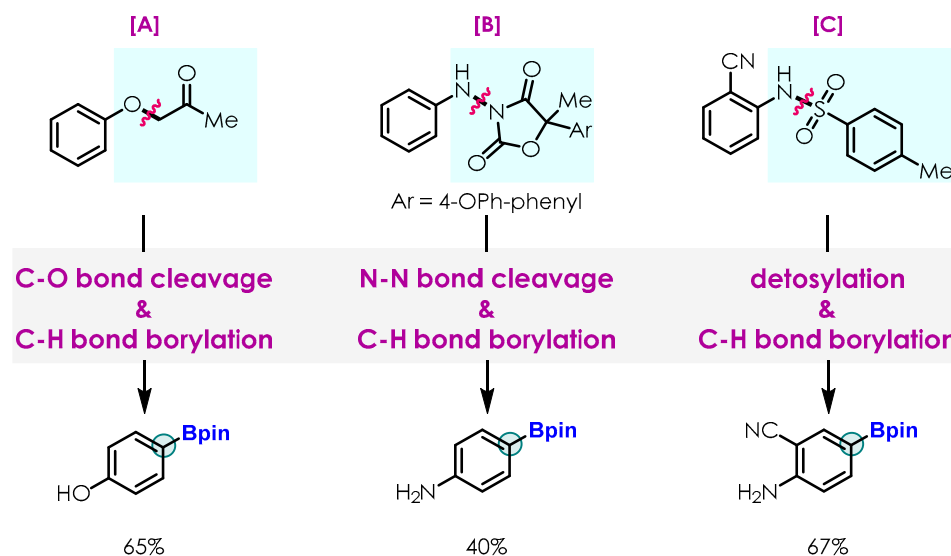

Figure 3. Novel cascade transformation. Reactions were performed with 0.2 mmol substrate, 1.0 mmol NH_4HCO_3, 20 mol% N-containing heterocycle (NCH), 0.8 mmol B_2Pin_2, 0.22 mmol NBS in 0.5 mL acetonitrile under 390 nm LEDs irradiation for 36 h, isolated yield. (**A**) Reductive C-O bond cleavage and C-H bond borylation. (**B**) Reductive N-N bond cleavage and C-H bond borylation. (**C**) Reductive N-S bond cleavage and C-H bond borylation.

3. Discussion

To gain more insight into the mechanism for this C-H bond borylation reaction, mechanistic and computational experiments were performed (Scheme 2). Scheme 2a shows that the N-methylacetanilide substrate cannot directly undergo the bromination reaction with NBS to afford N-(4-Bromophenyl)-N-methylacetamide without photoirradiation, and the borylation also cannot occur. However, the borylation of the N-methylacetanilide can occur under the standard condition, as well as under the condition where isoquinoline is replaced by complex **A** (complex **A** is formed by isoquinoline and B_2Pin_2) (Scheme 2b). Based on these observations, we infer that the arene substrate may interact with complex **B** (complex **A** + base) to form a new transient EDA complex, thereby being excited by visible light to increase the electron density of the arene, and then react with NBS and the diboron reagent to produce the borylation product. Density functional theory (DFT) calculations [48] show that the Gibbs free energy is uphill by 4.3 kcal/mol when complex **B** interacts with arene substrate via π–π stacking, indicating that the existence of the transient EDA complex is feasible (see Scheme 2c). Furthermore, the time-dependent DFT (TD-DFT) method was used to study the charge-transfer-type transitions of the transient EDA complex. The involved molecular orbitals (HOMO-1, HOMO and LUMO + 2) are depicted in Scheme 2d. Two significant excitations (HOMO-1 to LUMO + 2, and HOMO to LUMO + 2) can be assigned to the corresponding charge transfer from the complex **B** to the substrate, and the arene substrate with more electron density will facilitate the subsequent transformations.

[a]

[b]

[c]

[d]
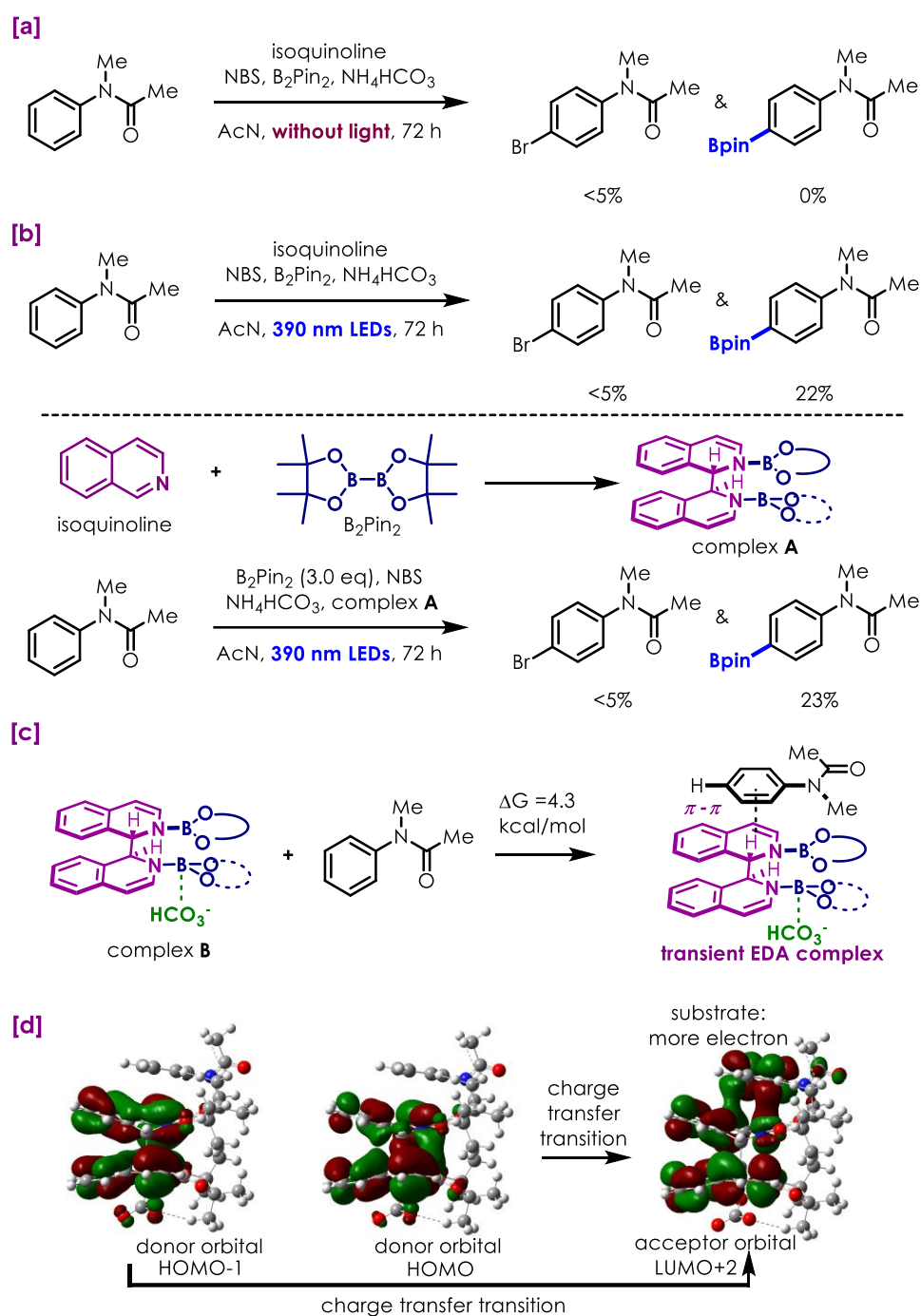
Scheme 2. Mechanistic and computational experiments: (**a**) mechanistic experiments using isoquino-line (0.04 mmol)/4-N-methylacetanilide (0.2 mmol)/NH$_4$HCO$_3$ (1.0 mmol)/B$_2$Pin$_2$ (0.8 mmol)/NBS (0.22 mmol) without 390 nm LEDs irradiation for 72 h; (**b**) mechanistic experiments using complex **A** (0.2 mmol)/4-N-methylacetanilide (0.2 mmol)/NH$_4$HCO$_3$ (1.0 mmol)/B$_2$Pin$_2$ (0.6 mmol)/NBS (0.22 mmol) with 2 × 390 nm LEDs irradiation for 72 h; (**c**) the binding Gibbs free energy between complex **B** and the arene substrate to form transient EDA complex; (**d**) TDDFT-computed donor and acceptor orbitals of charge transfer transitions in the transient EDA complex.

With these mechanistic insights, as well as the related literature, a plausible mechanism is proposed in Scheme 3. Complex **A**, generated through the reductive coupling of isoquinoline and B$_2$Pin$_2$, coordinates with the substrate and base to afford a transient EDA complex, which is then excited by 390 nm light, yielding a highly reactive excited

state. Oxidation by NBS may afford N-(4-Bromophenyl)-N-methylacetamide **C** (path b in Scheme 3) or directly afford aryl radical **D** (path a in Scheme 3) and regenerate complex **A**. Subsequently, aryl radical **D** could be trapped by the diboron reagent, furnishing the desired borylation products.
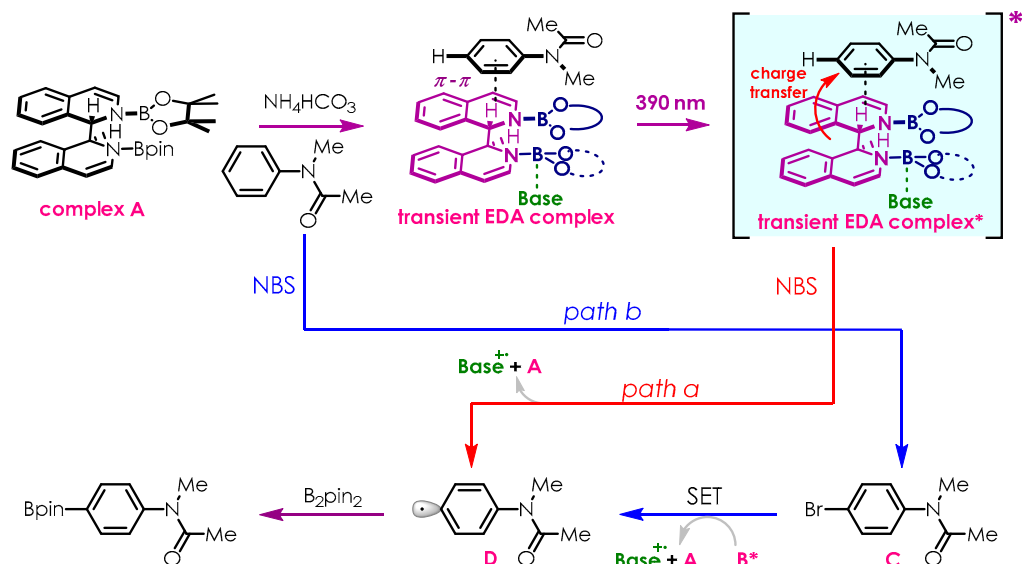
Scheme 3. The plausible mechanism. (The symbol * denotes excited state).

Compared with our previous reports of borylation methodologies, this concise strategy provides more efficient and a broader scope for aryl C-H bond borylation, achieved directly from simple arenes rather than the two-step one-pot synthesis from electron-rich arenes, presenting a new reaction mechanism.

4. Methods and Materials

4.1. Photo Reaction Setup

Irradiation of the photochemical reaction was carried out using Kessil PR160L-390 nm ultraviolet lamps from both sides at 1–2 cm, with an average intensity of 159 mW/cm^2 (measured from 6 cm distance). Reactions were cooled using a 20 W clamp fan placed on the top of the reactor. Stirring was achieved by placing the assembled reactor on IKA C-MAG HS 7 control magnetic stir bars. All reactions were performed in 2 mL vial and were run under air.

4.2. Thin-Layer Chromatography (TLC)

Analytical TLC was performed on silica gel GF254 plates. The TLC plates were visualized by ultraviolet light (λ = 254 nm). Organic solutions were concentrated using a rotary evaporator with a diaphragm vacuum pump purchased from EYELA and Heidolph. Fresh silica-gel chromatography was performed using 300–400 mesh silica gel (Qingdao, China).

4.3. Nuclear Magnetic Resonance Spectroscopy (NMR)

Proton and carbon magnetic resonance spectra (^{1}H NMR, ^{13}C NMR, ^{11}B NMR and ^{19}F NMR) were recorded on a Bruker AVANCE III (^{1}H NMR at 400 MHz or 600 MHz, ^{13}C NMR at 101 MHz or 151 MHz, ^{11}B NMR at 128 MHz or 193 MHz, ^{19}F NMR at 377 MHz) spectrometer, with solvent resonance as the internal standard (^{1}H NMR: CDCl$_3$ at 7.26 ppm; ^{13}C NMR: CDCl$_3$ at 77.16 ppm). NMR yield using pyrazine or hexamethyldisiloxane (HMDSO) was used as the internal standard.

4.4. Materials

Commercially available reagents were purchased from Sigma-Aldrich, Adamas-beta, TCI, and Bidepharm were used as received unless otherwise noted. Super Dry solvents such as acetonitrile (AcN), dimethylformamide (DMF), tetrahydrofuran (THF), dichloromethane (DCM), 1,2-dichloroethane (DCE) and dimethyl sulfoxide (DMSO) were purchased from Adamas-beta. Other common solvents such as petroleum ether (PE) and ethyl acetate (EtOAc) were rectification grade for flash chromatography on silica gel, purchased from General-reagent.

5. Conclusions

In summary, we have developed a novel diboron-type EDA-complex catalyzed C-H borylation of arenes, which occurs under ambient temperature and mild conditions. This operationally simple protocol exhibits exceptional regioselectivity and tolerates a wide range of functional groups, allowing convenient modification of complex natural products and APIs. Furthermore, the key role of the transient EDA complex formed in situ was confirmed through control experiments and computations, and a plausible mechanism was proposed. Perhaps even more useful, this method offers a versatile strategy to achieve novel one-pot multi-transformations, such as challenging reductive C-O/N-N/N-S bond cleavages followed by cascade aromatic C-H bond borylation.

Supplementary Materials: The following supporting information can be downloaded at: https://www.mdpi.com/article/10.3390/molecules29081783/s1. Scheme S1: Photo reaction setup; Table S1: Optimization of reaction conditions; Scheme S2: Substrates with low yield under optimized conditions; Scheme S3: Novel cascade transformation; Table S2: Oxidative additives screen and control experiments; Table S3: Reaction with complex A; Figures S1 and S2: The computational results; Tables S4–S7: Crystal data and structure refinement. References [49–85] are cited in Supplementary Materials.

Author Contributions: M.L. and L.W. discovered the reactions. M.L. performed the reaction optimizations and studied the reaction scope and synthetic utility with contributions from Q.C. and J.L. M.L. studied the reaction mechanisms. Y.-H.D., C.W. and T.-Y.S. performed the DFT calculations. T.-Y.S. and L.W. supervised the project. All authors have read and agreed to the published version of the manuscript.

Institutional Review Board Statement: Not applicable.

Informed Consent Statement: Not applicable.

Data Availability Statement: The data are contained in the article and Supplementary Materials.

Conflicts of Interest: The authors declare no conflicts of interest.

References

1. Miyaura, N.; Suzuki, A. Palladium-Catalyzed Cross-Coupling Reactions of Organoboron Compounds. *Chem. Rev.* **1995**, *95*, 2457–2483. [CrossRef]
2. Chemler, S.R.; Trauner, D.; Danishefsky, S.J. The B-Alkyl Suzuki–Miyaura Cross-Coupling Reaction: Development, Mechanistic Study, and Applications in Natural Product Synthesis. *Angew. Chem. Int. Ed.* **2001**, *40*, 4544–4568. [CrossRef]

3.   Lam, P.Y.S.; Clark, C.G.; Saubern, S.; Adams, J.; Winters, M.P.; Chan, D.M.T.; Combs, A. New aryl/heteroaryl C-N bond cross-coupling reactions via arylboronic acid/cupric acetate arylation. *Tetrahedron Lett.* **1998**, *39*, 2941–2949. [CrossRef]
4.   Antilla, J.C.; Buchwald, S.L. Copper-Catalyzed Coupling of Arylboronic Acids and Amines. *Org. Lett.* **2001**, *3*, 2077–2079. [CrossRef]
5.   West, M.J.; Fyfe, J.W.B.; Vantourout, J.C.; Watson, A.J.B. Mechanistic Development and Recent Applications of the Chan–Lam Amination. *Chem. Rev.* **2019**, *119*, 12491–12523. [CrossRef]
6.   Zou, Y.-Q.; Chen, J.-R.; Liu, X.-P.; Lu, L.-Q.; Davis, R.L.; Jørgensen, K.A.; Xiao, W.-J. Highly Efficient Aerobic Oxidative Hydroxylation of Arylboronic Acids: Photoredox Catalysis Using Visible Light. *Angew. Chem. Int. Ed.* **2012**, *51*, 784–788. [CrossRef]
7.   Wu, H.; Hynes, J. Copper-catalyzed chlorination of functionalized arylboronic acids. *Org. Lett.* **2010**, *12*, 1192–1195. [CrossRef]
8.   Petrone, D.A.; Ye, J.; Lautens, M. Modern Transition-Metal-Catalyzed Carbon-Halogen Bond Formation. *Chem. Rev.* **2016**, *116*, 8003–8104. [CrossRef]
9.   Fawcett, A.; Murtaza, A.; Gregson, C.H.U.; Aggarwal, V.K. Strain-Release-Driven Homologation of Boronic Esters: Application to the Modular Synthesis of Azetidines. *J. Am. Chem. Soc.* **2019**, *141*, 4573–4578. [CrossRef]
10. Letsinger, R.L.; Skoog, I.H. The preparation and some properties of 2-methyl-1-propene-1-boronic acid. *J. Org. Chem.* **1953**, *18*, 895–897. [CrossRef]
11. Légaré, M.; Rang, M.; Bélanger-Chabot, G.; Schweizer, J.I.; Krummenacher, I.; Bertermann, R.; Arrowsmith, M.; Holthausen, M.C.; Braunschweig, H. The reductive coupling of dinitrogen. *Science* **2019**, *363*, 1329–1332. [CrossRef] [PubMed]
12. Sherwood, J.; Clark, J.H.; Fairlamb, I.J.S.; Slattery, J.M. Solvent effects in palladium catalysed cross-coupling reactions. *Green Chem.* **2019**, *21*, 2164–2213. [CrossRef]
13. Partyka, D.V. Transmetalation of Unsaturated Carbon Nucleophiles from Boron-Containing Species to the Mid to Late d-Block Metals of Relevance to Catalytic C–X Coupling Reactions (X = C, F, N, O, Pb, S, Se, Te). *Chem. Rev.* **2011**, *111*, 1529–1595. [CrossRef] [PubMed]
14. Trouvé, J.; Gramage-Doria, R. Beyond hydrogen bonding: Recent trends of outer sphere interactions in transition metal catalysis. *Chem. Soc. Rev.* **2021**, *50*, 3565–3584. [CrossRef] [PubMed]
15. Chan, A.Y.; Perry, I.B.; Bissonnette, N.B.; Buksh, B.F.; Edwards, G.A.; Frye, L.I.; Garry, O.L.; Lavagnino, M.N.; Li, B.-X.; Liang, Y.; et al. Metallaphotoredox: The Merger of Photoredox and Transition Metal Catalysis. *Chem. Rev.* **2022**, *122*, 1485–1542. [CrossRef]
16. Lv, J.; Chen, X.; Xue, X.-S.; Zhao, B.; Liang, Y.; Wang, M.; Jin, L.; Yuan, Y.; Han, Y.; Zhao, Y.; et al. Metal-free directed sp2-C–H borylation. *Nature* **2019**, *575*, 336–340. [CrossRef] [PubMed]
17. Haldar, C.; Hoque, M.E.; Chaturvedi, J.; Hassan, M.M.M.; Chattopadhyay, B. Ir-catalyzed proximal and distal C-H borylation of arenes. *Chem. Commun.* **2021**, *57*, 13059–13074. [CrossRef] [PubMed]
18. Hu, J.; Ferger, M.; Shi, Z.-Z.; Marder, T.B. Recent advances in asymmetric borylation by transition metal catalysis. *Chem. Soc. Rev.* **2021**, *50*, 13129–13188. [CrossRef] [PubMed]
19. Bisht, R.; Haldar, C.; Hassan, M.M.M.; Hoque, M.E.; Chaturvedi, J.; Chattopadhyay, B. Metal-catalysed C–H bond activation and borylation. *Chem. Soc. Rev.* **2022**, *51*, 5042–5100. [CrossRef]
20. Börgel, J.; Ritter, T. Late-Stage Functionalization. *Chem* **2020**, *6*, 1877–1887. [CrossRef]
21. Zhang, L.; Ritter, T. A Perspective on Late-Stage Aromatic C–H Bond Functionalization. *J. Am. Chem. Soc.* **2022**, *144*, 2399–2414. [CrossRef] [PubMed]
22. Berger, F.; Ritter, T. Site-Selective Late-Stage C–H Functionalization via Thianthrenium Salts. *Synlett* **2022**, *33*, 339–345.
23. Mo, F.; Qiu, D.; Zhang, L.; Wang, J. Recent Development of Aryl Diazonium Chemistry for the Derivatization of Aromatic Compounds. *Chem. Rev.* **2021**, *121*, 5741–5829. [CrossRef] [PubMed]
24. Kvasovsa, N.; Gevorgyan, V. Contemporary methods for generation of aryl radicals. *Chem. Soc. Rev.* **2021**, *50*, 2244–2259. [CrossRef] [PubMed]
25. Berger, F.; Plutschack, M.B.; Riegger, J.; Yu, W.; Speicher, S.; Ho, M.; Frank, N.; Ritter, T. Site-selective and versatile aromatic C-H functionalization by thianthrenation. *Nature* **2019**, *567*, 223–228. [CrossRef] [PubMed]
26. Yu, X.-Y.; Chen, J.-R.; Xiao, W.-J. Visible Light-Driven Radical-Mediated C–C Bond Cleavage/Functionalization in Organic Synthesis. *Chem. Rev.* **2021**, *121*, 506–561. [CrossRef] [PubMed]
27. Bryden, M.A.; Zysman-Colman, E. Organic thermally activated delayed fluorescence (TADF) compounds used in photocatalysis. *Chem. Soc. Rev.* **2021**, *50*, 7587–7680. [CrossRef] [PubMed]
28. Holmberg-Douglas, N.; Nicewicz, D.A. Photoredox-Catalyzed C-H Functionalization Reactions. *Chem. Rev.* **2022**, *122*, 1925–2016. [CrossRef] [PubMed]
29. Beil, S.B.; Chen, T.Q.; Intermaggio, N.E.; MacMillan, D.W.C. Carboxylic Acids as Adaptive Functional Groups in Metallaphotoredox Catalysis. *Acc. Chem. Res.* **2022**, *55*, 3481–3494. [CrossRef]
30. Li, Q.; Liu, M.; Jiang, M.; Wan, L.; Ning, Y.; Chen, F.-E. Photo-induced 1,2-aryl migration of 2-chloro-1-arylpropanone under batch and flow conditions: Rapid, scalable and sustainable approach to 2-arylpropionic acids. *Chin. Chem. Lett.* **2024**, *35*, 108576. [CrossRef]
31. Han, Y.; Zhou, L.; Wang, C.; Feng, S.; Ma, R.; Wan, J.-P. Recent advances in visible light-mediated chemical transformations of enaminones. *Chin. Chem. Lett.* **2024**, *35*, 108977. [CrossRef]
32. Crisenza, G.E.M.; Mazzarella, D.; Melchiorre, P. Synthetic Methods Driven by the Photoactivity of Electron Donor-Acceptor Complexes. *J. Am. Chem. Soc.* **2020**, *142*, 5461–5476. [CrossRef]

33. Yuan, Y.-Q.; Majumder, S.; Yang, M.-H.; Guo, S.-R. Recent advances in catalyst-free photochemical reactions via electron-donor-acceptor (EDA) complex process. *Tetrahedron Lett.* **2021**, *61*, 151506. [CrossRef]

34. Yang, Z.; Liu, Y.; Cao, K.; Zhang, X.; Jiang, H.; Li, J. Synthetic reactions driven by electron-donor–acceptor (EDA) complexes. *Beilstein J. Org. Chem.* **2021**, *17*, 771–799. [CrossRef] [PubMed]

35. Van der Zee, L.J.C.; Pahar, S.; Richards, E.; Melen, R.L.; Chris Slootweg, J. Insights into Single-Electron-Transfer Processes in Frustrated Lewis Pair Chemistry and Related Donor–Acceptor Systems in Main Group Chemistry. *Chem. Rev.* **2023**, *123*, 9653–9675. [CrossRef] [PubMed]

36. Sandfort, F.; Strieth-Kalthoff, F.; Klauck, F.J.R.; James, M.J.; Glorius, F. Deaminative Borylation of Aliphatic Amines Enabled by Visible Light Excitation of an Electron Donor–Acceptor Complex. *Chem. Eur. J.* **2018**, *24*, 17210–17214. [CrossRef] [PubMed]

37. Wu, J.; He, L.; Noble, A.; Aggarwal, V.K. Photoinduced Deaminative Borylation of Alkylamines. *J. Am. Chem. Soc.* **2018**, *140*, 10700–10704. [CrossRef]

38. Wang, S.; Wang, H.; König, B. Photo-induced thiolate catalytic activation of inert Caryl-hetero bonds for radical borylation. *Chem* **2021**, *7*, 1653–1665. [CrossRef]

39. MacKenzie, I.A.; Wang, L.F.; Onuska, N.P.R.; Williams, O.F.; Begam, K.; Moran, A.M.; Dunietz, B.D.; Nicewicz, D.A. Discovery and characterization of an acridine radical photoreductant. *Nature* **2020**, *580*, 76–80. [CrossRef]

40. Li, M.; Liu, S.; Bao, H.; Li, Q.; Deng, Y.-H.; Sun, T.-Y.; Wang, L.F. Photoinduced metal-free borylation of aryl halides catalysed by an in situ formed donor–acceptor complex. *Chem. Sci.* **2022**, *3*, 4909–4914. [CrossRef]

41. Deng, Y.-H.; Li, Q.; Li, M.; Wang, L.F.; Sun, T.-Y. Rational design of super reductive EDA photocatalyst for challenging reactions: A theoretical and experimental study. *RSC Adv.* **2024**, *14*, 1902–1908. [CrossRef] [PubMed]

42. Zhang, L.; Jiao, L. Visible-Light-Induced Organocatalytic Borylation of Aryl Chlorides. *J. Am. Chem. Soc.* **2019**, *141*, 9124–9128. [CrossRef] [PubMed]

43. Liu, W.; Li, J.; Huang, C.-Y.; Li, C.-J. Aromatic Chemistry in the Excited State: Facilitating Metal-Free Substitutions and Cross-Couplings. *Angew. Chem. Int. Ed.* **2020**, *59*, 1786–1796. [CrossRef] [PubMed]

44. Zhu, Y.; Chen, S.; Zhou, Z.; He, Y.; Liu, Z.; Liu, Y.; Feng, Z. Iron/B$_2$pin$_2$ catalytic system enables the generation of alkyl radicals from inert alkyl C-O bonds for amien synthesis. *Chin. Chem. Lett.* **2024**, *35*, 108303. [CrossRef]

45. Liao, L.; Lin, D.; Histand, G. Visible light induced oxidative coupling of purines with arenes. *Chin. Chem. Lett.* **2023**, *34*, 107467. [CrossRef]

46. Nishii, Y.; Ikeda, M.; Hayashi, Y.; Kawauchi, S.; Miura, M. Triptycenyl Sulfide: A Practical and Active Catalyst for Electrophilic Aromatic Halogenation Using N-Halosuccinimides. *J. Am. Chem. Soc.* **2020**, *142*, 1621–1629. [CrossRef]

47. Song, S.; Li, X.; Wei, J.; Wang, W.; Zhang, Y.; Ai, L.; Zhu, Y.; Shi, X.; Zhang, X.; Jiao, N. DMSO-catalysed late-stage chlorination of (hetero)arenes. *Nat. Catal.* **2020**, *3*, 107–115. [CrossRef]

48. Frisch, M.J.; Trucks, G.W.; Schlegel, H.B.; Scuseria, G.E.; Robb, M.A.; Cheeseman, J.R.; Scalmani, G.; Barone, V.; Petersson, G.A.; Nakatsuji, H.; et al. *Gaussian 16*; Gaussian, Inc.: Wallingford, CT, USA, 2016.

49. Jin, S.-F.; Dang, H.T.; Haug, G.C.; He, R.; Nguyen, V.D.; Nguyen, V.T.; Arman, H.D.; Schanze, K.S.; Larionov, O.V. Visible Light-Induced Borylation of C–O, C–N, and C–X Bonds. *J. Am. Chem. Soc.* **2020**, *142*, 1603–1613. [CrossRef]

50. Chen, K.; Cheung, M.S.; Lin, Z.-Y.; Li, P.-F. Metal-free borylation of electron-rich aryl (pseudo)halides under continuous-flow photolytic conditions. *Org. Chem. Front.* **2016**, *3*, 875–879. [CrossRef]

51. McManus, J.B.; Nicewicz, D.A. Direct C–H Cyanation of Arenes via Organic Photoredox Catalysis. *J Am Chem Soc.* **2017**, *139*, 2880–2883. [CrossRef]

52. Uetake, Y.; Niwa, T.; Hosoya, T. Rhodium-Catalyzed ipso-Borylation of Alkylthioarenes via C–S Bond Cleavage. *Org. Lett.* **2016**, *18*, 2758–2761. [CrossRef] [PubMed]

53. Mir, R.; Dudding, T. Phase-Transfer Catalyzed O-Silyl Ether Deprotection Mediated by a Cyclopropenium Cation. *J. Org. Chem.* **2017**, *82*, 709–714. [CrossRef] [PubMed]

54. Nitelet, A.; Thevenet; Schiavi, B.; Hardouin, C.; Fournier, J.; Tamion, R.; Pannecoucke, X.; Jubault, P.; Poisson, T. Copper-Photocatalyzed Borylation of Organic Halides under Batch and Continuous-Flow Conditions. *Chem. -Eur. J.* **2019**, *25*, 3262–3266.

55. Gong, Y.-X.; Zhu, Z.-D.; Qian, Q.; Tong, W.-Q.; Gong, H.-G. Miyaura Borylation and One-Pot Two-Step Homocoupling of Aryl Chlorides and Bromides under Solvent-Free Conditions. *Org. Lett.* **2021**, *23*, 1005–1010. [CrossRef] [PubMed]

56. Dzhevakov, P.B.; Topchiy, M.A.; Zharkova, D.A.; Morozov, O.S.; Asachenko, A.F.; Nechaev, M.S. Miyaura Borylation and One-Pot Two-Step Homocoupling of Aryl Chlorides and Bromides under Solvent-Free Conditions. *Adv. Synth. Catal.* **2016**, *358*, 977–983. [CrossRef]

57. Wei, D.; Sadek, O.; Dorcet, V.; Roisnel, T.; Darcel, C.; Gras, E.; Clot, E.; Sortais, J.-B. Selective mono N-methylation of anilines with methanol catalyzed by rhenium complexes: An experimental and theoretical study. *J. Catal.* **2018**, *366*, 300–309. [CrossRef]

58. Firth, J.D.; Hammarback, L.A.; Burden, T.J.; Eastwood, J.B.; Donald, J.R.; Horbaczewskyj, C.S.; McRobie, T.; Tramaseur, A.; Clark, I.P.; Towrie, M.; et al. Light- and Manganese-Initiated Borylation of Aryl Diazonium Salts: Mechanistic Insight on the Ultrafast Time-Scale Revealed by Time-Resolved Spectroscopic Analysis. *Chem. Eur. J.* **2020**, *27*, 3979–3985.

59. Yamamoto, T.; Morita, T.; Takagi, J.; Yamakawa, T. NiCl2(PMe3)2-Catalyzed Borylation of Aryl Chlorides. *Org. Lett.* **2011**, *12*, 5766–5769.

60. Gisbertz, S.; Reischauer, S.; Pieber, B. Overcoming limitations in dual photoredox/nickel-catalysed C–N cross-couplings due to catalyst deactivation. *Nat. Catal.* **2020**, *3*, 611–620.

61. Guerrand, H.D.S.; Marciasini, L.D.; Jousseaume, M.; Vaultier, M.; Pucheault, M. Borylation of Unactivated Aryl Chlorides under Mild Conditions by Using Diisopropylaminoborane as a Borylating Reagent. *Chem. Eur. J.* **2014**, *20*, 5573–5579. [CrossRef]

62. Dong, J.; Guo, H.; Hu, Q.-S. Room Temperature Ni0/PCy3-Catalyzed Coupling Reactions of Aryl Arenesulfonates with Bis(pinacolato)diboron. *Eur. J. Org. Chem.* **2017**, *2017*, 7087–7090. [CrossRef]

63. Waring, M.J.; Birch, A.M.; Birtles, S.; Buckett, L.K.; Butlin, R.J.; Campbell, L.; Gutierrez, P.M.; Kemmitt, P.D.; Leach, A.G.; MacFaul, P.A.; et al. Optimisation of biphenyl acetic acid inhibitors of diacylglycerol acetyl transferase 1—the discovery of AZD2353. *Med. Chem. Commun.* **2013**, *4*, 159–164. [CrossRef]

64. Preshlock, S.M.; Plattner, D.L.; Maligres, P.E.; Krska, S.W.; Maleczka J, R.E.; Smith, M.R., II. A Traceless Directing Group for C-H Borylation. *Angew. Chem. Int. Ed.* **2013**, *52*, 12915–12919. [CrossRef]

65. Qiu, D.; Wang, S.; Tang, S.-B.; Meng, H.; Jin, L.; Mo, F.-Y.; Zhang, Y.; Wang, J.-B. Synthesis of Trimethylstannyl Arylboronate Compounds by Sandmeyer-Type Transformations and Their Applications in Chemoselective Cross-Coupling Reactions. *J. Org. Chem.* **2014**, *79*, 1979–1988. [CrossRef] [PubMed]

66. Mihai, M.T.; Williams, B.D.; Phipps, R.J. Para-Selective C–H Borylation of Common Arene Building Blocks Enabled by Ion-Pairing with a Bulky Countercation. *J. Am. Chem. Soc.* **2019**, *141*, 15477–15482. [CrossRef] [PubMed]

67. Taylor, N.J.; Emer, E.; Preshlock, S.; Schedler, M.; Tredwell, M.; Verhoog, S.; Mercier, J.; Genicot, C.; Gouverneur, V. Derisking the Cu-Mediated ^{18}F-Fluorination of Heterocyclic Positron Emission Tomography Radioligands. *J. Am. Chem. Soc.* **2017**, *139*, 8267–8276. [CrossRef] [PubMed]

68. Kong, C.; Jana, N.; Jones, C.; Driver, T.G. Control of the Chemoselectivity of Metal N-Aryl Nitrene Reactivity: C–H Bond Amination versus Electrocyclization. *J. Am. Chem. Soc.* **2016**, *138*, 13271–13280. [CrossRef]

69. Inglis, S.R.; Woon, E.C.Y.; Thompson, A.L.; Schofield, C.J. Observations on the Deprotection of Pinanediol and Pinacol Boronate Esters via Fluorinated Intermediates. *J. Org. Chem.* **2010**, *75*, 468–471. [CrossRef] [PubMed]

70. Clary, J.W.; Rettenmaier, T.J.; Snelling, R.; Bryks, W.; Banwell, J.; Wipke, W.T.; Singaram, B. Hydride as a Leaving Group in the Reaction of Pinacolborane with Halides under Ambient Grignard and Barbier Conditions. One-Pot Synthesis of Alkyl, Aryl, Heteroaryl, Vinyl, and Allyl Pinacolboronic Esters. *J. Org. Chem.* **2011**, *76*, 9602–9610. [CrossRef] [PubMed]

71. Zernickel, A.; Du, W.-Y.; Ghorpade, S.A.; Sawant, D.N.; Makki, A.A.; Sekar, N.; Eppinger, J. Bedford-Type Palladacycle-Catalyzed Miyaura Borylation of Aryl Halides with Tetrahydroxydiboron in Water. *J. Org. Chem.* **2018**, *83*, 1842–1851. [CrossRef] [PubMed]

72. Davalos, A.R.; Sylvester, E.; Diver, S.T. Macrocyclic N-Heterocyclic Carbenes: Synthesis and Catalytic Applications. *Organometallics.* **2019**, *38*, 2338–2346. [CrossRef]

73. Chapman, T.M.; Osborne, S.A.; Wallace, C.; Birchall, K.; Bouloc, N.; Jones, H.M.; Ansell, K.H.; Taylor, D.L.; Clough, B.; Green, J.L.; et al. Optimization of an Imidazopyridazine Series of Inhibitors of Plasmodium falciparum Calcium-Dependent Protein Kinase 1 (PfCDPK1). *J. Med. Chem.* **2014**, *57*, 3570–3587. [CrossRef]

74. Lyu, H.-R.; Kevlishvili, I.; Yu, X.; Liu, P.; Dong, G.-B. Boron insertion into alkyl ether bonds via zinc/nickel tandem catalysis. *Science* **2021**, *372*, 175–182. [CrossRef]

75. Yin, Q.; Klare, H.F.T.; Oestreich, M. Catalytic Friedel–Crafts C−H Borylation of Electron-Rich Arenes: Dramatic Rate Acceleration by Added Alkenes. *Angew. Chem. Int. Ed.* **2017**, *56*, 3712–3717. [CrossRef] [PubMed]

76. Lv, Y.-C.; Li, M.-Y.; Liu, T.; Tong, L.-J.; Peng, T.; Wei, L.-X.; Ding, J.; Xie, H.; Duan, W.-H. Discovery of a New Series of Naphthamides as Potent VEGFR-2 Kinase Inhibitors. *ACS Med. Chem. Lett.* **2014**, *5*, 592–597. [CrossRef] [PubMed]

77. Chen, D.-P.; Xu, G.-Q.; Zhou, Q.-H.; Chung, L.-W.; Tang, W.-J. Practical and Asymmetric Reductive Coupling of Isoquinolines Templated by Chiral Diborons. *J. Am. Chem. Soc.* **2017**, *139*, 9767–9770.

78. Zhao, Y.; Truhlar, D.G. The M06 suite of density functionals for main group thermochemistry, thermochemical kinetics, noncovalent interactions, excited states, and transition elements: Two new functionals and systematic testing of four M06-class functionals and 12 other functionals. *Theor. Chem. Acc.* **2008**, *120*, 215–241.

79. Weigend, F.; Ahlrichs, R. Balanced basis sets of split valence, triple zeta valence and quadruple zeta valence quality for H to Rn: Design and assessment of accuracy. *Phys. Chem. Chem. Phys.* **2005**, *7*, 3297–3305. [CrossRef] [PubMed]

80. Clark, T.; Chandrasekhar, J.; Spitznagel, G.W.; Schleyer, P.V. Efficient diffuse function-augmented basis sets for anion calculations. III.† The 3-21+G basis set for first-row elements, Li–F. *J. Comput. Chem.* **1983**, *4*, 294–301. [CrossRef]

81. Tomasi, J.; Mennucci, B.; Cammi, R. Quantum Mechanical Continuum Solvation Models. *Chem. Rev.* **2005**, *105*, 2999–3094. [CrossRef]

82. Adamo, C.; Jacquemin, D. The calculations of excited-state properties with Time-Dependent Density Functional Theory. *Chem. Soc. Rev.* **2013**, *42*, 845–856. [CrossRef] [PubMed]

83. Dolomanov, O.V.; Bourhis, L.J.; Gildea, R.J.; Howard, J.A.K.; Puschmann, H.J. OLEX2: A complete structure solution, refinement and analysis program. *J. Appl. Cryst.* **2009**, *42*, 339–341. [CrossRef]

84. Sheldrick, G.M. SHELXT—Integrated space-group and crystalstructure determination. *Acta Cryst.* **2015**, *A71*, 3–8.

85. Sheldrick, G.M. Crystal structure refinement with SHELXL. *Acta Cryst.* **2015**, *C71*, 3–8.